Redox Biology 67 (2023) 102923

Contents lists available at ScienceDirect

Redox Biology

journal homepage: www.elsevier.com/locate/redox

Cancer-associated fibroblasts impair the cytotoxic function of NK cells in gastric cancer by inducing ferroptosis via iron regulation

Lizhong Yao [1], Junyi Hou [1], Xiongyan Wu, Yifan Lu, Zhijian Jin, Zhenjia Yu, Beiqin Yu, Jianfang Li, Zhongyin Yang, Chen Li, Min Yan, Zhenggang Zhu, Bingya Liu, Chao Yan [**], Liping Su [*]

Department of General Surgery, Shanghai Key Laboratory of Gastric Neoplasms, Shanghai Institute of Digestive Surgery, Ruijin Hospital, Shanghai Jiao Tong University School of Medicine, Shanghai, 200025, China

A R T I C L E I N F O

Keywords:
Cancer-associated fibroblasts
NK cells
Iron regulation
Ferroptosis
Ferritinophagy

A B S T R A C T

As the predominant immunosuppressive component within the tumor microenvironment (TME), cancer-associated fibroblasts (CAFs) inhibit Natural Killer cell (NK cell) activity to promote tumor progression and immune escape; however, the mechanisms of cross-talk between CAFs and NK cells in gastric cancer (GC) remain poorly understood. In this study, we demonstrate that NK cell levels are inversely correlated with CAFs abundance in human GC. CAFs impair the anti-tumor capacity of NK cells by inducing ferroptosis, a cell death process characterized by the accumulation of iron-dependent lipid peroxides. CAFs induce ferroptosis in NK cells by promoting iron overload; conversely, decreased intracellular iron levels protect NK cells against CAF-induced ferroptosis. Mechanistically, CAFs increase the labile iron pool within NK cells via iron export into the TME, which is mediated by the upregulated expression of iron regulatory genes ferroportin1 and hephaestin in CAFs. Moreover, CAF-derived follistatin like protein 1(FSTL1) upregulates NCOA4 expression in NK cells via the DIP2A-P38 pathway, and NCOA4-mediated ferritinophagy is required for CAF-induced NK cell ferroptosis. In a human patient-derived organoid model, functional targeting of CAFs using a combination of deferoxamine and FSTL1-neutralizing antibody significantly alleviate CAF-induced NK cell ferroptosis and boost the cytotoxicity of NK cells against GC. This study demonstrates a novel mechanism of suppression of NK cell activity by CAFs in the TME and presents a potential therapeutic approach to augment the immune response against GC mediated by NK cells.

1. Introduction

Gastric cancer (GC) is a primary malignant tumor that poses a significant health burden globally and was the fourth cause of cancer-related death in 2020 [1]. Neoadjuvant chemoradiotherapy followed by radical gastrectomy is the main treatment for the disease, though the overall prognosis for patients with unresectable GC is dismal, mainly due to metastasis and recurrence. Therefore, elucidating the underlying mechanisms in GC progression and identifying novel therapeutic strategies are urgent.

Previous work suggests that a high intra-tumoral stroma proportion is closely associated with the poor prognosis of GC [2,3]. Cancer-associated fibroblasts (CAFs), which constitute the primary stromal cell population within the tumor microenvironment (TME), are intimately involved in the growth and metastasis of GC [4]. An intricate crosstalk between CAFs and immune cells establishes an immune-suppressive microenvironment that supports tumor progression [5,6]. CAFs facilitate immune evasion by suppressing the cytotoxic activity of Natural killer cells (NK cells), an innate immune cell population that constitutes a first line defense against cancer. While NK cells can eliminate malignant cells in a non-specific manner, their activity is regulated by a delicate balance between activating and inhibitory signals [7–10]. Increased understanding of the intricacies of NK cell biology has facilitated the utilization of NK cells in cancer treatments,

* Corresponding author.
** Corresponding author.
E-mail addresses: yanchaosuper@163.com (C. Yan), suliping@shsmu.edu.cn (L. Su).
[1] Lizhong Yao and Junyi Hou contributed equally to this article.

https://doi.org/10.1016/j.redox.2023.102923
Received 19 September 2023; Accepted 4 October 2023
Available online 6 October 2023

including chimeric antigen receptor (CAR)-NK cell therapy [10,11]. Nevertheless, the efficacy of NK cell-based therapies for solid tumors remains unsatisfactory, primarily due to the immune-suppressive effects of the TME [12–14]. Tumor stromal cells, infiltrating immunosuppressive cells, or tumor cells within the TME impair NK cell cytotoxic function through direct cell-to-cell contact or release of soluble mediators, including cytokines. CAF-secreted factors such as indoleamine-pyrrole 2,3-dioxygenase, matrix metalloproteinases, and prostaglandin E2 suppress NK cell-mediated elimination of solid tumors [15,16]. Although the cross-talk between CAFs and NK cells is known to exert major inhibitory effects on NK cell activity, the interaction between CAFs and NK cells in GC remains poorly understood. In this study, we demonstrate that NK cell levels are inversely correlated with CAFs abundance in human GC. CAFs impair the anti-tumor capacity of NK cells by inducing ferroptosis, a process characterized by the accumulation of iron-dependent lipid peroxides [17]. Mechanistically, CAFs increase labile iron within NK cells by exporting iron into the TME and also induce NCOA4-mediated ferritinophagy via CAF-derived Follistatin Like Protein 1 (FSTL1). A combination of deferoxamine (DFO) and FSTL1-neutralizing antibody significantly alleviates CAF-induced NK cell ferroptosis and boosts the cytotoxicity of NK cells against GC, which constitutes a potentially effective therapeutic strategy to enhance the antitumor immune response in GC.

2. Materials and methods

2.1. Cell lines and patient samples

SNU16, MKN45, and NK92 cell lines were purchased from ATCC. All cells were authenticated using short tandem repeat analysis and were verified to be negative for mycoplasma contamination. Gastric CAFs and normal fibroblasts (NFs) were isolated and cultured as described [18]. SNU16 and MKN45 cells were cultured in RPMI-1640 medium containing 10 % FBS. NK92 cells were cultured in alpha-minimum essential medium supplemented with 12.5 % FBS, 12.5 % horse serum, 0.02 mmol folic acid, 0.2 mmol inositol, 0.1 mmol beta-mercaptoethanol, and 500 IU/mL IL-2 at 37 °C in a humidified atmosphere of 5 % CO_2. Samples from GC patients who underwent radical gastrectomy were obtained with informed consent at Shanghai Ruijin Hospital and were histologically confirmed. The reagents were listed in Table S1.

2.2. Isolation of NK cells from peripheral blood mononuclear cells (pb-NK cells)

Pb-NK cells were isolated and enriched through indirect magnetic immunoselection (Miltenyi, Germany, 130-092-657) and cultured in NK MACS medium (Miltenyi, Germany, 130-114-429) supplemented with 1 % NK MACS supplement, 500 IU/ml IL-2, and activation beads (Miltenyi, Germany, 130-094-483). The cells were incubated for a minimum of 7 days until the $CD56^{+}CD3^{-}$ NK cell population reached approximately 90 %, as confirmed by flow cytometry (Fig. S1A).

2.3. CAFs and NK cell co-culture

CAFs and pb-NK/NK92 cells (2:1 ratio) were co-cultured indirectly using 6-well plate inserts or 24-well plate inserts. After 48 h, pb-NK/NK92 cells were collected and utilized for subsequent analyses.

2.4. NK cell cytotoxicity assays

NK cell cytotoxicity was assessed using DELFIA EuTDA cell cytotoxicity assays (PerkinElmer, USA, AD0116). MKN45 and SNU16 cells were labeled with BATDA for 30 min at 37 °C and then washed with PBS. Subsequently, pb-NK cells and NK92 cells were added to the BATDA-labeled MKN45 and SNU16 cells in 96-well V-bottom plates at 20:1, 10:1, 5:1, and 2.5:1 effector/target (E:T) cell ratios. The plates were incubated for 4 h, and 20 μl of supernatant and 200 μl of Europium solution were then added to a flat-bottom plate. Fluorescence was measured in a time-resolved fluorometer.

2.5. Flow cytometric analysis

Pb-NK cells and NK92 cells were stained with immunofluorescence-conjugated antibodies (listed in Table S1). Data were acquired using a FACS Calibur cytometer and analyzed using CellQuest software.

2.6. Cell viability assay

NK cells or CAFs were plated in 24-well plates or 96-well plates and Cell Counting Kit-8 (Dojindo,Japan,CK04) reagent was added and the cell viability was quantified by measuring the absorbance at 450 nM on a microplate reader (Epoch; BioTek, Winooski, VT).

2.7. Quantitative real-time PCR (qRT-PCR)

Total RNA was extracted using Trizol reagent (Invitrogen, USA). RNA (1 ug) was reverse transcribed into cDNA using the Reverse Transcription system (Promega, USA) and was quantified using the SYBR Green PCR core Reagent kit (Applied Biosystems, USA) with validated primers (Table S2). Data were analyzed by the comparative Ct method.

2.8. Western blotting

Western blotting was performed as described previously [19]. Membranes were immunoblotted with the indicated primary and secondary antibodies (listed in Table S1), and were visualized with Thermo Pierce Blots chemiluminescent (ECL) Immunoblot-ting Substrate (Thermo, Waltham, MA, USA) using a Tanon 5200 system (Tanon, Shanghai, China).

2.9. Enzyme-linked immunosorbent assay

Concentrations of soluble cytokines and 4-Hydroxynonenal (4-HNE) in samples were determined by enzyme-linked immunosorbent assay (ELISA). The protein levels of IFN-y, TNF-α or FSTL1 in the supernatants of cells were measured by human sandwich ELISA kit (listed in Table S1) according to the manufacturer's protocols. The levels of 4-HNE in cells were measured by human competitive ELISA kit(listed in Table S1)according to the manufacturer's protocols.

2.10. Lipid malondialdehyde (MDA) and reactive oxygen species (ROS) assays

MDA levels were measured using a MDA Assay Kit (Dojindo, Japan, M496). The reaction mixture was evaluated on a fluorescence microplate reader (Safire2, Tecan, Switzerland) and MDA levels were expressed as nmol/mg protein. For ROS analysis, cells were stained with 2 uM BODIPY 581/591 C11 (Abclonal, USA, RM02821) for 30 min at 37 °C and then washed three times with PBS. The fluorescence was measured using a fluorescence microplate reader.

2.11. Labile iron pool and total iron assays

The labile iron pool in NK92 cells was measured using FerroOrange (Dojindo Japan, F374). Cells were washed three times with HBSS, and then 1 μM FerroOrange was added for 30 min at 37 °C. The samples were sealed under SB-Shifix coverslips (ShikharBiotech, Nepal), and the fluorescence was measured on a fluorescence microplate reader.

Iron ions in fibroblasts were measured using Calcein-AM (MedChemExpress, USA, HY-D0041). Cells were collected and washed twice with PBS and then incubated with 0.125 μmol/L Calcein-AM for 15 min at 37 °C. The fluorescence was measured using a fluorescence microplate

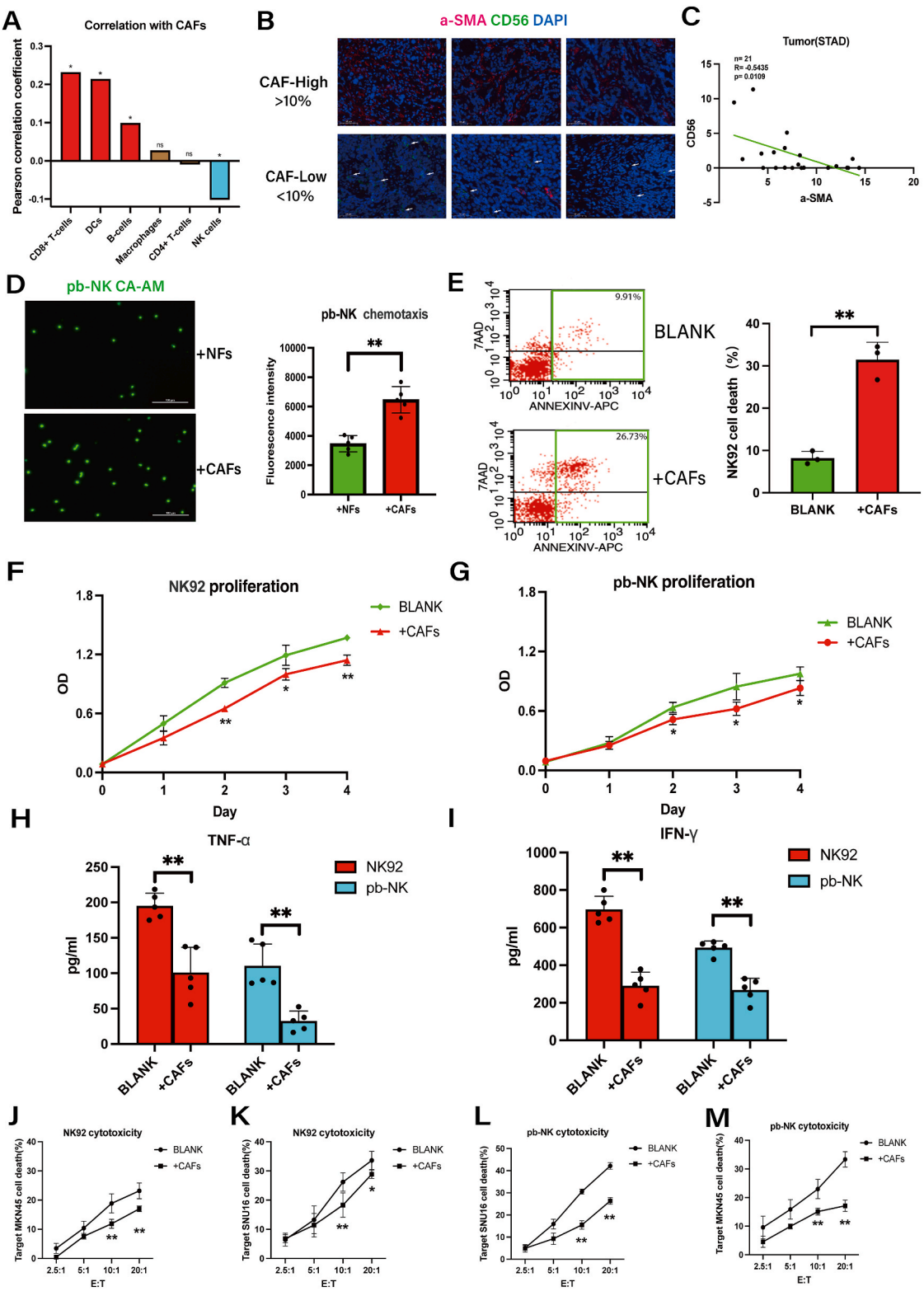

Fig. 1. CAFs levels are inversely correlated with NK cells levels in human gastric cancer and inhibit NK cells viability and cytotoxicity in vitro.
A, The correlation of immune cells and CAFs in GC tissues according to the TCGA database. B–C, Representative immunofluorescence staining of α-SMA and CD56 in GC tumor tissues and the correlation of α-SMA and CD56 in 21 GC tumor tissues Arrows indicate the expression of CD56 (scale bar = 50um). D, Chemotaxis of pb-NK cells (labeled with Calcein-AM) induced by NFs and CAFs was determined by fluorescence intensity assay. E, Flow cytometry assessment of cell death for NK92 cells cultured alone (BLANK) or co-cultured with CAFs. F-G, The proliferation of NK92/pb-NK cells co-cultured with CAFs was measured by CCK8 assay. H–I, Protein levels of TNF-a and IFN-y secreted by NK92/pb-NK cells co-cultured with CAFs were measured by ELISA. J-M, The effects of CAFs on NK92 and pb-NK cytotoxicity against SNU16 and MKN45 GC cells were measured by DELFIA EuTDA cell cytotoxicity assay. Data are representative of at least three independent experiments. Student t-test and pearson correlation analysis were used to analyze the data (mean ± SD; *P < 0.05, **P < 0.01).

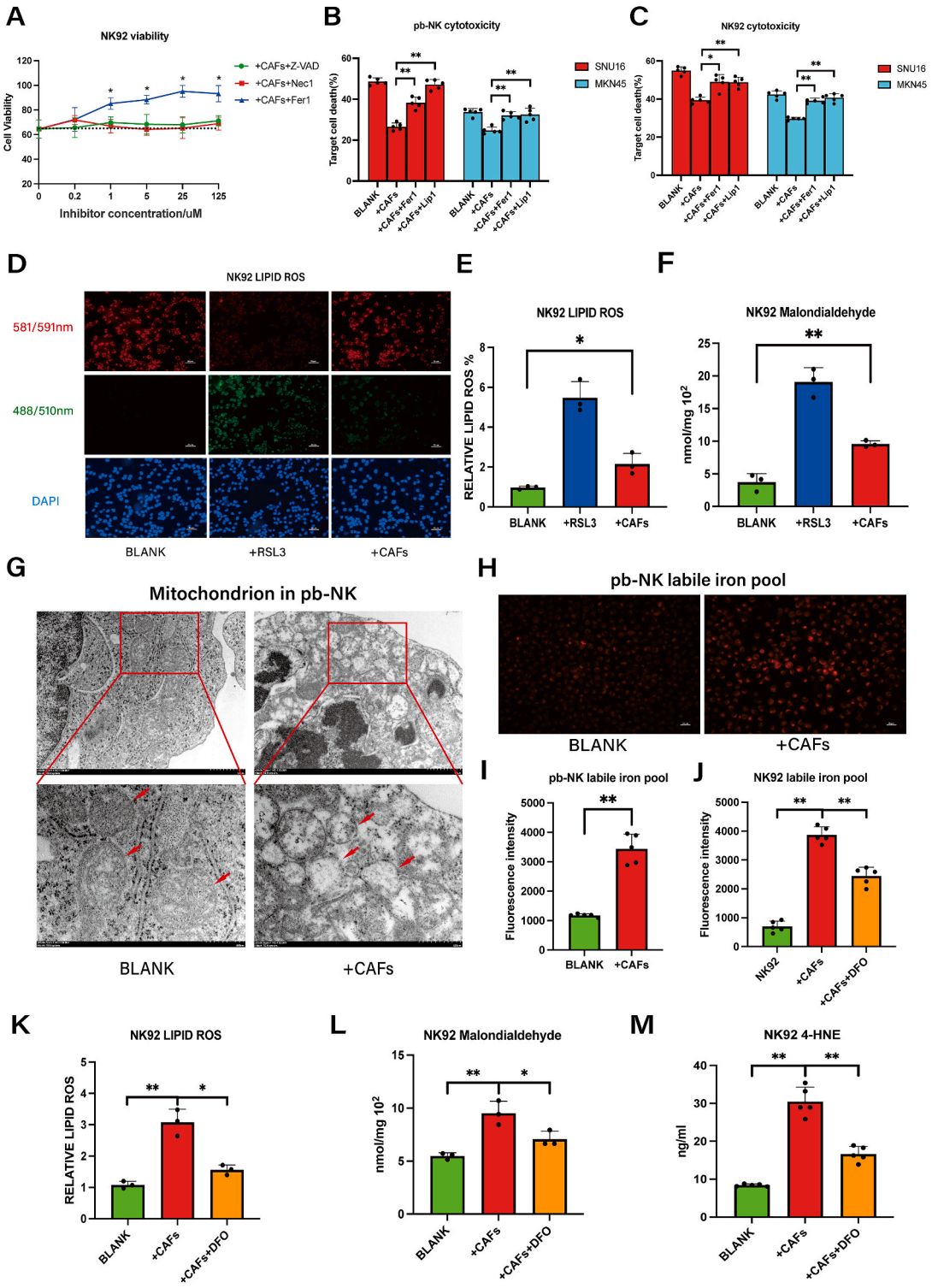

Fig. 2. CAFs induce ferroptosis by promoting intracellular iron overload in NK cells.
A, The viability of NK92 cells co-cultured with CAFs was measured by CCK8 assay in the presence of specific inhibitors Z-VAD (caspase-3 inhibitor), Nec1 (necroptosis inhibitor), or Fer1 (ferroptosis inhibitor) for 48 h. B–C, The effects of CAFs on NK92 and pb-NK cytotoxicity against MKN45 and SNU16 GC cells were measured by DELFIA EuTDA cell cytotoxicity assay (Fer1 5 μM, Lip1 50 nM). D-E, Lipid ROS in NK92 cells co-cultured with CAFs was detected using C11 BODYPI 581/591 probe. NK92 cells treated with 0.5 μM RSL3 for 48 h served as a positive control (scale bar = 20um). F, MDA in NK92 cells co-cultured with CAFs was detected using an MDA assay kit. NK92 cells treated with 0.5 μM RSL3 for 48 h served as a positive control. G, The mitochondria of pb-NK cells were analyzed by transmission electron microscopy (scale bar = 1μm/500 nm). H–I, Ferrous iron in pb-NK cells was detected by ferroorange assay in untreated cells or co-culture with CAFs (+CAFs) (scale bar = 20um). J, Ferrous iron in NK92 cells was detected by ferroorange assay in untreated cells after co-culture with CAFs in the absence or presence of DFO (10 μM, 48 h). K, Lipid ROS in NK92 cells co-cultured with CAFs only or CAFs plus DFO (10 μM) was detected by C11 BODYPI 581/591 probe. L, MDA in NK92 cells co-cultured with CAFs only or CAFs plus DFO (10 μM) was detected by MDA assay. M, 4-HNE in NK92 cells co-cultured with CAFs only or CAFs plus DFO (10 μM) was detected by ELISA. Data are representative of at least three independent experiments. Student t-test was used to analyze the data (mean ± SD; *P < 0.05, **P < 0.01).

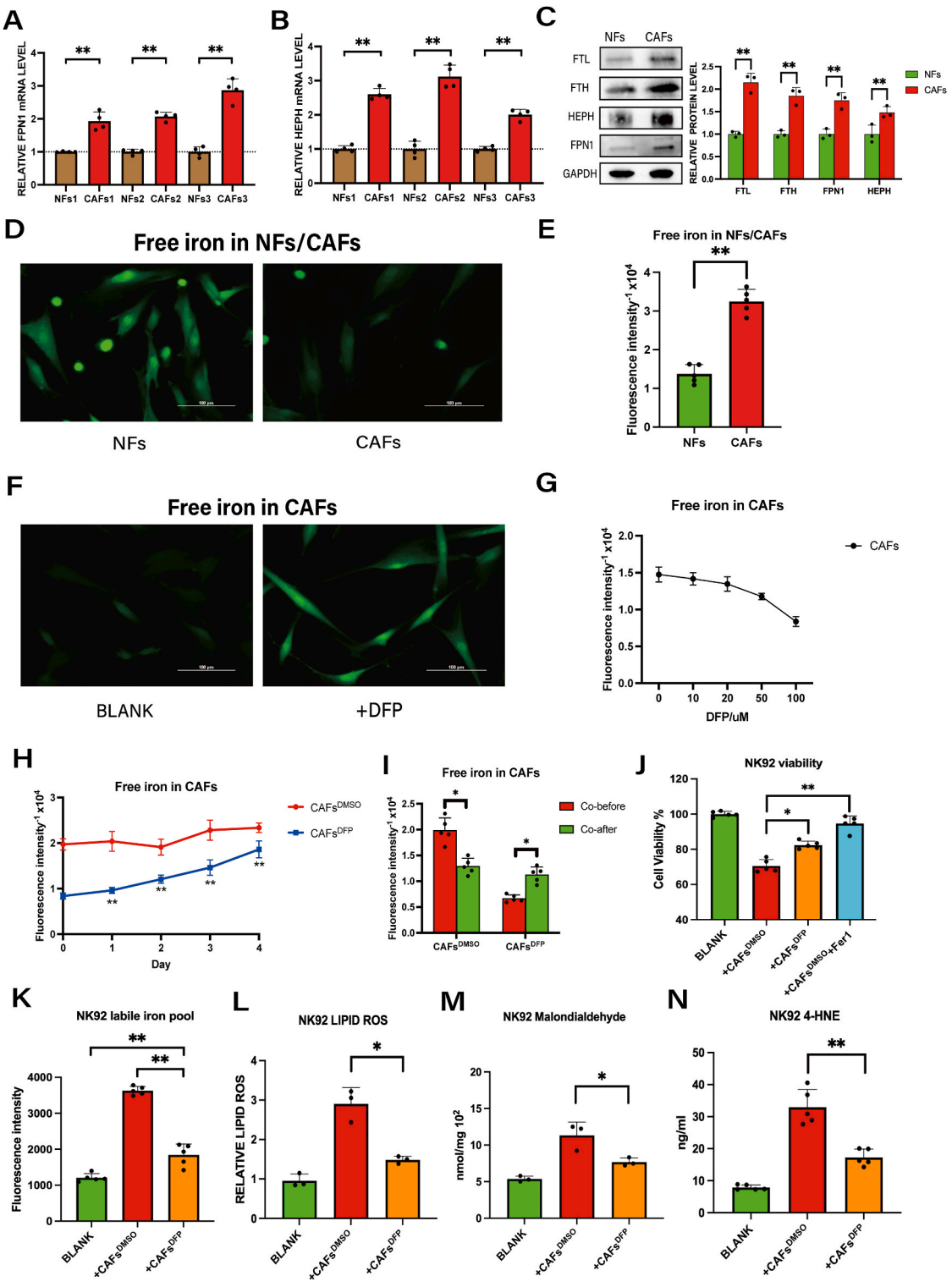

Fig. 3. CAFs elevate NK cell labile iron pool levels via iron export into the TME.
A-B, The mRNA levels of hephaestin (HEPH) and ferroportin1 (FPN1) in three pairs of normal fibroblasts (NFs) and CAFs were analyzed by QRT-PCR. C, Protein expression of FTH, FTL, FPN1 and HEPH in NFs versus CAFs was analyzed by western blot assay. D-E, Iron ions in NFs and CAFs were detected by Calcein-AM staining (scale bar = 100um). F-G, Iron ions in CAFs were detected by Calcein-AM staining after treatment with indicted doses of DFP (0–100 μM, 48 h) (scale bar = 100um). H, Changes in iron ions within CAFs after removal of DFP were detected by Calcein-AM. I, Iron ions in CAFs only or CAFs plus DFP co-cultured with NK92 was detected by Calcein-AM. J, The viability of NK92 cells co-cultured with CAFs only or CAFs plus DFP was measured by CCK8 assay (Fer1:5 μM). K, Ferrous iron in NK92 cells co-cultured with CAFs only or CAFs plus DFP (100 μM) was detected by ferroorange assay. The fluorescence was measured on a fluorescence microplate reader. L, Lipid ROS in NK92 cells co-cultured with CAFs only or CAFs plus DFP (100 μM) was detected by C11 BODYPI 581/591 probe. M, MDA in NK92 cells co-cultured with CAFs only or CAFs plus DFP (100 μM) was detected by MDA assay. N, 4-HNE in NK92 cells co-cultured with CAFs only or CAFs plus DFP (100 μM) was detected by ELISA. Data are representative of at least three independent experiments. Student t-test was used to analyze the data (mean ± SD; *P < 0.05, **P < 0.01).

reader. Given that CA-AM fluorescence intensity increases as the free iron content decreases, the reciprocal of fluorescence intensity was taken as the number of free iron ions.

2.12. Establishment of MSLN-CAR-92 cells

MSNL-CAR is composed of the MSNL antibody variable region (scfv), the CD8 hinge and transmembrane region, 4-BB co-stimulatory molecule, and CD3-ζ sequences. The scfv sequence was acquired from a public patent (WO 2022/135578 A1), while the remaining sequences were obtained via the NCBI database. The CAR sequence was synthetized and cloned into the pLVX-IRES-ZsGreen1 lentiviral vector, which was introduced into Stbl3 E. coli receptor cells, followed by amplification and culturing of monoclones. Endotoxin-free plasmid was prepared for subsequent experimentation using the MN Plasmid Extraction Kit (CWBIO, China, CW2105).

To prepare genetically engineered NK cells, the CAR-expressing shuttle vector, psPAX2 packaging vector, and pMD2.G packing vector were transfected into HEK293T cells. Lentiviral supernatants were collected at 48 h, 72 h and 96 h, and virus was concentrated using the Universal Virus Concentration Kit (Beyotime, China, C2901S). NK92 cells were transduced with MOI 200 of MSLN-CAR lentivirus and 5 μg/ml polybrene. The transfection efficiency was verified by flow cytometry.

2.13. CAR-NK92 cytotoxicity assays

Patient-derived organoids (PDOs) from GC were established and cultured as described [19]. To establish a co-culture model, PDOs were combined with CAFs and NK92 or CAR-NK92 cells at a 1:2:5 ratio under various conditions, including the addition of DFO and FSTL1-neutralizing antibody, for 48 h using 24-well plate inserts to enable indirect cell-cell contact. To evaluate the efficacy of CAR-NK92 cells, PDO1T was labeled with CytoTell650 (AAT Bioquestand, USA, 22255) assessed by flow cytometry; additionally, PDO3T was treated with Calcein-blue-AM (MedChemExpress, USA, HY-124298) and visualized using fluorescence microscopy. The ROI of images was analyzed using ImageJ software and calculated after subtracting the background signal.

2.14. Statistical analysis

All experiments were repeated at least three times, and the results were presented as means ± SD. Student t-test and pearson correlation analysis were used to analyze the data. P values < 0.05 were regarded as statistically significant differences ($^*P < 0.05$, $^{**}P < 0.01$).

3. Results

3.1. CAFs are inversely correlated with NK cell levels in human GC and inhibit NK cell viability and cytotoxicity in vitro

To investigate the association between CAFs and immune cells in GC, we analyzed their relative abundances using the TCGA database (Fig. S1B). Intriguingly, only NK cell levels exhibited a negative correlation with CAFs abundance (Fig. 1A). Next, we analyzed the levels of CAFs and NK cells in 21 pairs of GC tissues by immunofluorescence staining. As shown in Fig. 1B-C, the levels of a-SMA$^+$CAFs and CD56$^+$NK cells showed an inverse correlation. To provide a potential explanation for the inverse correlation, we conducted chemotaxis experiments on pb-NK cells using NFs and CAFs as stimuli for 8 h (Fibroblasts: NK = 2:1). In contrast to the above findings, CAFs demonstrated a more pronounced chemotactic effect on NK cells when compared to NFs (Fig. 1D). However, upon co-culture with CAFs, NK cells exhibited remarkably reduced cell viability (Fig. 1E) and cell proliferation (Fig. 1F–G) and CAFs proliferation was not affected by NK cells (Fig. S1D). Consistently, in NK cell functional assays, pretreatment with CAFs did not alter the expression of NK cells' activating or inhibitory receptors (Fig. S1C). However, it impaired the ability of NK cells to secrete cytokines (Fig. 1H–I) and exert cytotoxicity against gastric cancer (GC) cells (Fig. 1J-M). Therefore, these findings suggested that CAFs impede both NK cell viability and cytotoxicity, with the decline in cytotoxicity potentially resulting from a decrease in cell viability.

3.2. CAFs induce NK cell ferroptosis by promoting intracellular iron overload

To further evaluate the mechanism of CAFs in suppressing NK cell viability in GC, we performed CCK8 cell viability analysis. As shown in Fig. 2A, CAF-induced NK cell death was reversed by the ferroptosis inhibitor Ferrostatin-1 (Fer-1), but not by inhibitors of apoptosis (Z-VAD) or necroptosis (Nec-1). Furthermore, CAF-induced impairment of NK cell cytotoxicity against GC cells was partially restored by Fer-1 and Lip-1(another ferroptosis inhibitor) (Fig. 2B–C). Ferroptosis is known to be triggered by excessive lipid peroxidation and dysregulated intracellular iron [17]. Consistently, CAF-induced cell death in NK92 cells was accompanied by significant increases in intracellular lipid ROS and MDA (Fig. 2D–F). Transmission electron microscopy unveiled the presence of wrinkled mitochondria, membrane ruptures, and a reduction in mitochondrial cristae in pb-NK cells subsequent to co-culture with CAFs (Fig. 2G). The ferrous iron in pb-NK cells also increased after co-culturing with CAFs (Fig. 2H–I). To determine whether increased ferrous iron is a direct cause of ferroptosis, we pre-treated NK92 cells with the iron chelator DFO [20]. As shown in Figs. 2J and 10 μM DFO eliminated the excess iron from NK92 cells without negatively impacting the cellular activity of NK cells or CAFs (Fig. S2A); additionally, pre-treatment with 10 μM DFO resulted in reduced levels of CAF-induced ROS, MDA and 4-HNE in NK92 cells (Fig. 2K-M). Collectively, these results indicate that CAFs provoke iron overload to induce ferroptosis in NK cells.

3.3. CAFs elevate the level of NK cell labile iron pools by exporting iron into the TME

Dysregulated iron metabolism is a hallmark of many cancers [21,22] and is manifested as iron overload in the TME [23,24]. Therefore, we hypothesized that CAFs may provide iron to cancer cells or immune cells within the TME to facilitate ferroptosis. To address this possibility, we examined the expression of iron metabolism-related proteins in CAFs. Our findings confirm higher mRNA and protein levels of the iron export proteins ferroportin1 (FPN1) [25] and hephaestin (HEPH) [26] and higher protein levels of the iron storage protein ferritin (FTL and FTH) in CAFs compared to NFs (Fig. 3A–C). We also observed elevated total iron (Fig. 3D–E), indicating that CAFs have increased iron storage and export capacity within the TME of GC.

To determine whether iron overload derived from CAFs can induce ferroptosis in NK92 cells, we treated CAFs with the intracellular iron chelator deferiprone (DFP) [27] for 48 h. As shown in Fig. 3F-G, 100 μM DFP significantly decreased the intracellular iron levels in CAFs without affecting CAFs viability (Fig. S2B). Because treatment of NK92 cells with 100 μM DFP induced cell death (Fig. S2B) and the levels of iron ions within CAFs did not show a significant increase after a 2-day period of DFP removal (Fig. 3H), we performed a two-step procedure in which we first treated CAFs with 100 μM DFP and then removed the DFP prior to subsequent co-culture with NK92 cells. As shown in Fig. 3I, DFP-untreated CAFs exhibited a reduction in intracellular iron ions following co-culture with NK92, whereas DFP-treated CAFs demonstrated an increase in iron ions after co-culture with NK92. The result indicated that DFP-treated cancer-associated fibroblasts (CAFs) lost their ability to export iron to NK cells. At the same time, DFP-treatment of CAFs significantly increased NK92 cells viability (Fig. 3J) and decreased the levels of ferrous iron, ROS, MDA and 4-HNE in co-cultured

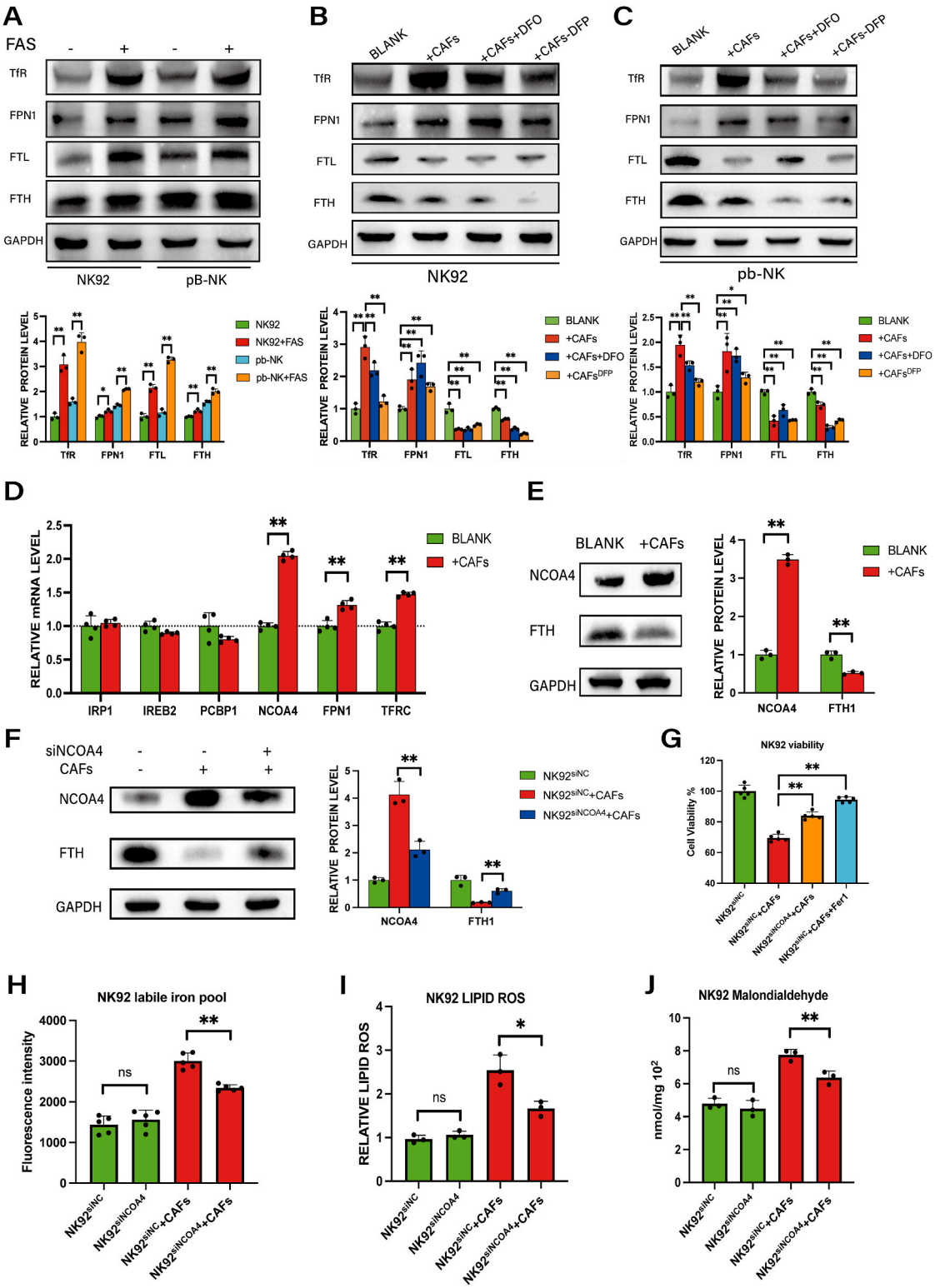

Fig. 4. Ferritinophagy via NCOA4 is involved in CAF-induced intracellular iron overload in NK cells.
A, Protein expression of TfR, FPN1, FTL and FTH in pb-NK and NK92 cells after incubation with FAS (100 μM) was analyzed by western blotting. B–C, Western blotting analysis of TfR, FPN1, FTL and FTH in pb-NK and NK92 cells co-cultured with CAFs, with CAFs and DFO (10 μM), or with DFP (100 μM)-pre-treated CAFs. D, The mRNA levels of genes associated with ferritin regulation in NK92 cells after co-culture with CAFs were analyzed by QRT-PCR. E, Western blotting of NCOA4 and FTH in NK92 cells co-cultured with CAFs. F, Western blotting of NCOA4 and FTH in NK92siNC or NK92siNCOA4 cells co-cultured with CAFs. G, The viability of NK92siNC or NK92siNCOA4 co-cultured with CAFs was measured by CCK8 assay (Fer1 5 μM). H, Ferrous iron in NK92siNC or NK92siNCOA4 cultured with or without CAFs was detected by ferroorange assay. I, Lipid ROS was detected by C11 BODYPI 581/591 probe. J, MDA was detected by MDA assay. Data are representative of at least three independent experiments. Student t-test was used to analyze the data (mean ± SD; *P < 0.05, **P < 0.01).

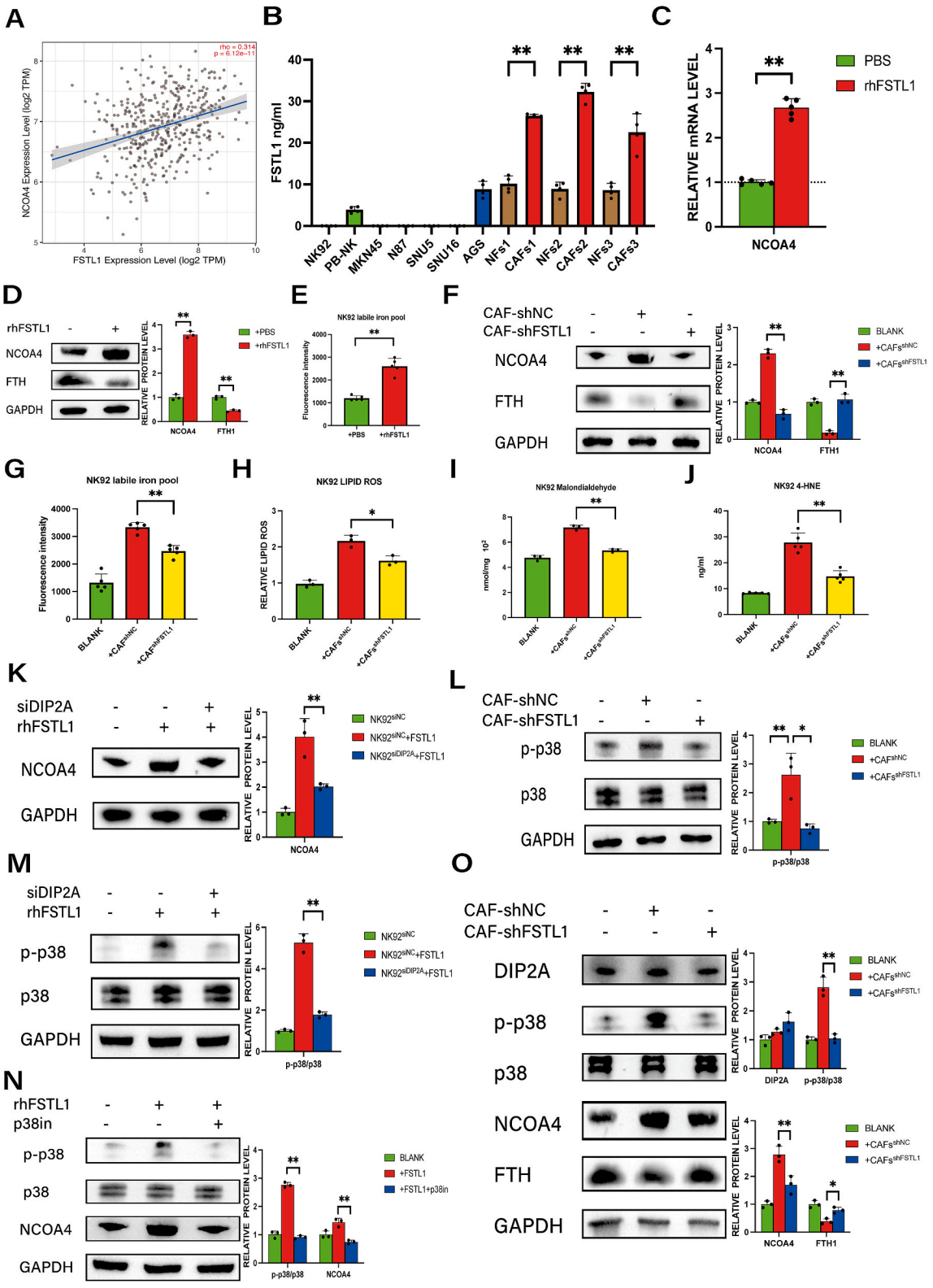

(caption on next page)

Fig. 5. CAF-derived FSTL1 upregulates NCOA4 expression in NK cells via the DIP2A-P38 pathway.
A, The correlation between NCOA4 and FSTL1 expression in GC from TCGA database. B, The FSTL1 concentration in cell supernatants from NK cells (pb-NK, NK92), GC cell lines (MKN-45, N87, SNU5, SNU16, and AGS) and paired NF and CAFs from GC patients was analyzed by ELISA. C, The mRNA level of NCOA4 in NK92 cells treated with rhFSTL1 (20 ng/ml) for 48 h were analyzed by QRT-PCR. D, Protein expression of NCOA4 and FTH in NK92 cells treated with rhFSTL1 (20 ng/ml; 48 h) was analyzed by western blotting. E, Ferrous iron in NK92 cells treated with or without rhFSTL1 (20 ng/ml; 48 h) was detected by ferroorange assay. F, Protein expression of NCOA4 and FTH in NK92 cells co-cultured with CAFs-shFSTL1 or CAFs-shNC for 48 h was analyzed by western blotting. G, Ferrous iron in NK92 cells co-cultured with CAFs-shFSTL1 or CAFs-shNC for 48 h was detected by ferroorange assay. H, Lipid ROS in NK92 cells co-cultured with CAFs-shFSTL1 or CAFs-shNC was detected using C11 BODYPI 581/591 probe. I, MDA in NK92 cells co-cultured with CAFs-shFSTL1 or CAFs-shNC was detected by MDA assay. J, 4-HNE in NK92 cells co-cultured with CAFs-shFSTL1 or CAFs-shNC was detected by ELISA. K, Protein expression of NCOA4 in NK92siDIP2A or control cells treated with rhFSTL1 (20 ng/ml; 48 h) was analyzed by western blotting. L, Protein expression of p-p38 and p38 in NK92 cells co-cultured with CAFs-shFSTL1 or CAFs-shNC was analyzed by western blotting. M, Protein expression of p-p38 and p38 in NK92siDIP2A or control cells treated with rhFSTL1 (20 ng/ml; 48 h) was analyzed by western blotting. N, Protein expression of p-p38, p38 and NCOA4 in NK92 cells treated with rhFSTL1 (20 ng/ml) or p38 inhibitor (p38-MAPK-in-1 20 μM) was analyzed by western blotting. O, Protein expression of DIP2A, p-p38, p38, NCOA4 and FTH in pb-NK cells co-cultured with CAFs-shFSTL1 or CAFs-shNC was analyzed by western blotting. Data are representative of at least three independent experiments. Student t-test and pearson correlation analysis were used to analyze the data (mean ± SD; *P < 0.05, **P < 0.01).

NK92 cells (Fig. 3K-N). These results further support a mechanism in which CAFs induce ferroptosis by elevating the labile iron pool in NK cells through iron export.

3.4. NCOA4-dependent ferritinophagy mediates CAF-induced intracellular iron overload in NK cells

To further investigate the regulatory mechanism of CAFs regulating NK cell viability in GC, we analyzed the cell viability and quantified the expression of iron metabolism-related proteins, including transferrin receptor (TFR) [28], FPN1 [25], FTL and FTH [29], in NK cells after adding of iron to the medium. As shown in Fig. 4A and Fig. S3A, the addition of iron led to significant upregulation of each of these proteins but also reduced NK cells viability (Fig. S3B). Co-culture with CAFs promoted a similar upregulation of TFR and FPN1 expression in NK cells, whereas the addition of DFO or pre-treatment of CAFs with DFP suppressed these increases. However, co-culture with CAFs dramatically downregulated FTL and FTH expression in NK cells (Fig. 4B–C). The latter finding is surprising given the role of ferritin in iron storage [29] and raises the possibility that degradation of ferritin may serve to enhance the accumulation of labile iron in NK cells. Thus, to verify the effect of CAFs on ferritin, we analyzed the mRNA levels of genes associated with ferritin regulation. Consistent with the western blotting results, co-culture with CAFs upregulated the expression of both FPN1 and TFR. Notably, nuclear receptor coactivator 4 (NCOA4), a selective cargo receptor in the autophagic degradation of ferritin (i.e., ferritinophagy) [30], also was significantly upregulated in NK92 cells after co-culture with CAFs (Fig. 4D). Furthermore, western blot analysis corroborated the downregulation of FTH and upregulation of NCOA4 in NK92 cells upon co-culture with CAFs (Fig. 4E).

To verify that the upregulation of NCOA4 is responsible for ferritin degradation, we knocked down NCOA4 expression in NK92 cells (Fig. S3C). For co-cultures with CAFs, NCOA4 silencing abolished ferritin degradation in NK92 cells (Fig. 4F). Furthermore, co-cultured NK92 cells with NCOA4 knockdown had increased cells viability (Fig. 4G) and reduced levels of ferrous iron (Fig. 4H), lipid ROS (Fig. 4I) and MDA (Fig. 4J); these effects were dependent on CAFs co-culture, thus verifying the role of CAFs in promoting NCOA4-induced ferritinophagy.

3.5. CAF-derived FSTL1 upregulates NCOA4 expression in NK cells via the DIP2A-P38 pathway

In the above assessments, NK cells were co-cultured with CAFs using an indirect system, suggesting that CAFs increase NCOA4 expression in NK cells via soluble factors. To screen for factors from CAFs that mediate in the upregulation of NCOA4, we performed mass spectrometry analysis of CAFs supernatants and analyzed the top 50 secreted proteins in the TCGA database. The results revealed a positive correlation between NCOA4 and FSTL1 [31], a secreted glycoprotein that contributes to inflammatory and malignant phenotypes across various cancers (Fig. S4), including GC (Fig. 5A). We performed qPCR and ELISA to further quantify the expression of FSTL1 in three pairs of CAFs and NFs, as well as NK cells and GC cell lines. As shown in Fig. S5A and Fig. 5B, FSTL1 mRNA and secreted FSTL1 in cell supernatants were significantly higher in CAFs than in NFs or GC cells.

To further assess the role of FSTL1 in NCOA4-mediated ferritinophagy induced by CAFs, we stimulated NK92 cells with recombinant human FSTL1 (rhFSTL1) for 48 h. The results demonstrate that rhFSTL1 upregulated NCOA4 in NK92 cells at both the transcriptional (Fig. 5C) and protein (Fig. 5D) levels. Moreover, rhFSTL1 reduced the levels of FTH protein, which is consistent with the increased ferrous iron levels occurring via ferritin degradation (Fig. 5E).

As additional evidence for the role of FSTL1 in NK92 ferritinophagy, we knocked down endogenous FSTL1 in CAFs using lentivirus (Figs. S5B–C) and then co-cultured shNC-CAFs or shFSTL1-CAFs with NK92 cells. As shown in Fig. 5F-G, FSTL1 knockdown resulted in decreases in NCOA4 expression and iron levels in NK92 cells. Moreover, the levels of ROS, MDA and 4-HNE were significantly decreased in NK92 cells co-cultured with shFSTL1-CAFs as compared to shNC-CAFs (Fig. 5H–J). These data suggest that FSTL1 secreted by CAFs induces NCOA4-mediated ferritinophagy and ferroptosis in NK cells.

To further elucidate the mechanisms by which FSTL1 upregulates NCOA4 expression in NK cells, we investigated potential receptors for FSTL1 in NK92 cells [31–34]. Our results indicate that NK92 cells express CD14 and DIP2A, but not TLR4 and BMP4 (Fig. S6A). To evaluate the roles of these receptors, we used siRNAs to knock down endogenous expression in NK92 cells (Figs. S6B–C). Silencing of CD14 expression had minimal effect on the upregulation of NCOA4 induced by rhFSTL1 (Fig. S6D); however, siDIP2A prevented rhFSTL1 from upregulating NCOA4 protein expression (Fig. 5K), indicating that FSTL1 may regulate NCOA4 expression in NK92 cells by binding to DIP2A.

To further assess FSTL1 signaling mechanisms, we evaluated pathways known to be triggered by FSTL1 [31,35–39] or involved in ferritinophagy [40,41](Fig. S7). Our results demonstrate that the p38 pathway in NK92 cells was activated after co-culture with CAFs but was reduced by shFSTL1 (Fig.5L). Furthermore, activation of the p38 pathway by rhFSTL1 was dependent on DIP2A (Fig.5M). To further determine whether the p38 pathway modulates NCOA4 in NK92 cells, we used a specific inhibitor to attenuate p38 signaling after rhFSTL1 treatment. Inhibition of the p38 pathway significantly decreased the expression of NCOA4 (Fig.5N). To validate these results in pb-NK cells, we established co-cultures with CAF-shNC or CAF-shFSTL. As shown in Fig.5O, the expression of NCOA4 and phosphorylation of p38 was increased, and the expression of FTH was decreased, upon co-culture with CAF-shNC; notably, FTSL1 knockdown in CAFs attenuated these effects. Together, these data indicate that CAF-derived FSTL1 upregulates NCOA4 expression in NK cells via the DIP2A-p38 pathway.

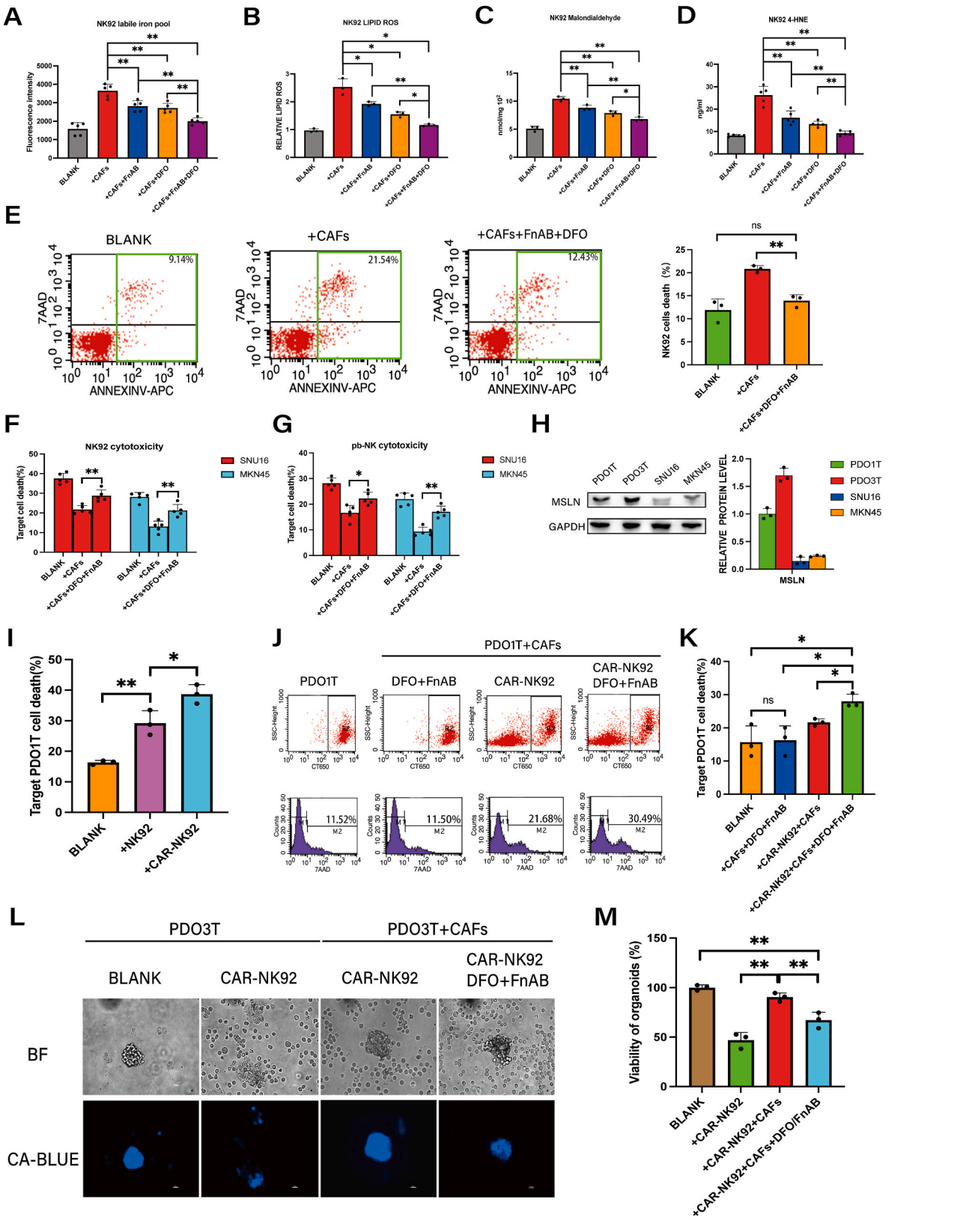

(caption on next page)

Fig. 6. Combined application of DFO and FSTL1-neutralizing antibody alleviates CAF-induced NK cell ferroptosis and boosts the cytotoxicity of NK cells against GC. A, Ferrous iron in NK92 cells co-cultured with CAFs with or without FSTL1-neutralizing antibody (FnAB, 1 μg/ml) and/or DFO (10 μM) was detected by ferroorange assay. B, Lipid ROS in NK92 cells co-cultured with CAFs with or without FnAB (1 μg/ml) and DFO (10 μM) was detected by C11 BODYPI 581/591 probe. C, MDA in NK92 cells co-cultured with CAFs with or without FSTL1-neutralizing antibody (FnAB, 1 μg/ml) and DFO (10 μM) was detected by MDA assay. D, 4-HNE in NK92 cells co-cultured with CAFs with or without FSTL1-neutralizing antibody (FnAB, 1 μg/ml) and DFO (10 μM) was detected by ELISA.E, The cell death of NK92 cells co-cultured with CAFs with or without FnAB (1 μg/ml) and DFO (10 μM) was analyzed by flow cytometry. F-G, The cytotoxicity of NK92 cells and pb-NK against MKN45 and SNU16 GC cells was measured by DELFIA EuTDA cell cytotoxicity assay after co-culture with CAFs with or without FnAB (1 μg/ml) and DFO (10 μM). H, Protein expression of MSLN in GC organoids (PDO1T and PDO3T) and GC cells (MKN45 and SNU16) was analyzed by western blotting. I, The cell death of PDO1T co-cultured with NK92 or CAR-NK cells (PDO1T: NK92 or CAR-NK = 1:5) was analyzed by flow cytometry. J-K, The cell death of PDO1T co-cultured with CAFs in the presence of DFO/FnAB and/or CAR-NK cells (PDO1T: CAFs: NK = 1:2:5, DFO: 10 μM, FnAB: 1 μg/ml) was analyzed by flow cytometry. L-M The cell death of PDO3T co-cultured with CAFs in the presence of DFO/FnAB and/or CAR-NK cells (PDO1T: CAFs: NK = 1:2:5, DFO: 10 μM, FnAB: 1 μg/ml) was analyzed by Calcein-blue-AM(scale bar = 20um). The data are presented as the mean ± SD from three independent experiments. Student t-test was used to analyze the data (*P < 0.05; **P < 0.01). (For interpretation of the references to colour in this figure legend, the reader is referred to the Web version of this article.)

3.6. Combined application of DFO and FSTL1-neutralizing antibody alleviates CAF-induced NK cell ferroptosis and boosts the cytotoxicity of CAR-NK against GC

To assess whether interventions targeting iron and FSTL1 mitigate CAF-induced ferroptosis in NK cells, we added DFO and/or FSTL1-neutralizing antibody (FnAB) to the NK92/CAFs coculture system. Each intervention had some effectiveness on its own, but the combination displayed greater efficacy in reducing the labile iron pool, as well as ROS, MDA and 4-HNE levels, in NK92 cells (Fig. 6A–D). Flow cytometry analysis revealed that combined application of DFO/FnAB almost completely reversed the death of NK92 cells induced by CAFs (Fig. 6E). Furthermore, with an effector-to-target (E:T) ratio of 10:1, combined DFO/FnAB application partially restored the cytotoxicity of NK92 cells and pb-NK cells towards GC cells in co-cultures (Fig. 6F–G).

To further evaluate the therapeutic potential of DFO and FnAB against GC, we developed CAR-NK92 cells specifically targeting Mesothelin (MSLN) (Fig. S8A), a cell-surface glycoprotein that is overexpressed in solid cancers [42], including GC (Fig. 6H). Additionally, we developed MSLN-positive patient-derived organoids (PDOs [43–45]), for evaluating MSLN-CAR-NK92 cells (Fig. S8B and Fig. 6I). Consistent with the above findings, combined treatment with DFO and FnAB enhanced MSLN-CAR-NK92 cell-mediated cancer killing in a PDO1T/-CAFs co-culture system (Fig. 6J–K). To further validate the therapeutic effect, we employed another MSLN + GC PDO (PDO3T), which was treated with Calcein-blue-AM dye and visualized using fluorescence microscopy. Notably, the combination of DFO and FnAB treatment promoted a substantial increase in CAR-NK92 cell-mediated killing (Fig. 6L–M). Therefore, the combination of FSTL1-neutralizing antibody and DFO treatment may present a promising therapeutic strategy for overcoming tumor stroma-mediated immune suppression in GC.

4. Discussion

Cancer progression involves genetic alterations of cancer cells and remodeling of the TME, including altered matrix architecture and immunosuppressive phenotypes that favor tumor growth, metastasis and immune evasion [2–6]. NK cells play a significant role in innate immune defenses, including their cytotoxicity against malignant cells [8]; however, their responses are significantly hindered by the

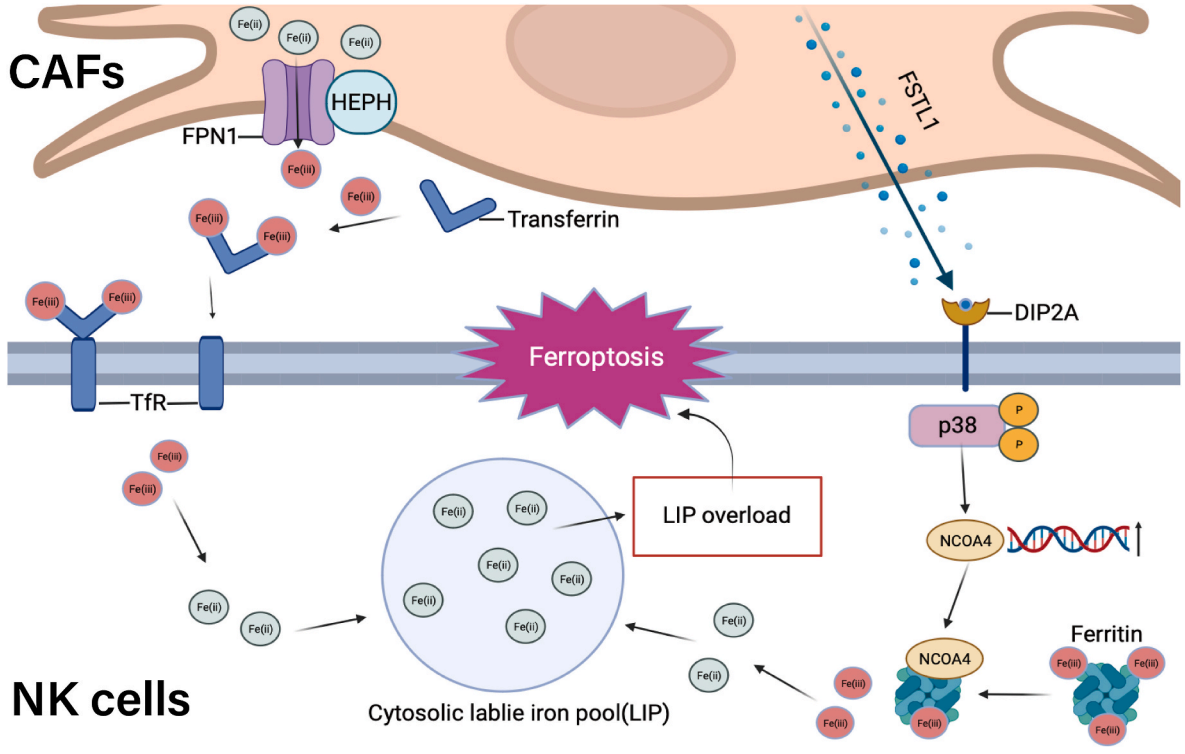

Fig. 7. Schematic representation of the putative mechanism by which CAFs induce NK cell ferroptosis in GC.
CAFs increase labile iron within NK cells to induce ferroptosis by exporting iron into TME and also induce FSTL1-NCOA4-mediated ferritinophagy in GC. Therefore, incorporating FSTL1-neutralizing antibody and DFO treatment may present a promising therapeutic strategy to treat GC by overcoming the immune suppression from the tumor stroma.

immunosuppressive effects from TME stromal components [15]. Here, we describe a new mechanism of tumor stroma-mediated regulation of NK cell function in GC. Our results indicate that the main component of tumor stroma, CAFs, increase iron overload to induce ferroptosis in NK cells, which impairs the anti-tumor immune response.

Cytotoxic activity in NK cells is regulated by a dynamic interplay between inhibitory and activating signals originating from the plasma membrane, and CAFs modulate these signals to impair NK cell-mediated anti-tumor responses. Previous studies have demonstrated that CAFs significantly decrease NKG2D expression on NK cells [46,47]. The phenotype and functions of NK cells are influenced both by direct cell contact and by soluble immunomodulators [16]. Our results define a new mode of regulation of NK cells, whereby CAFs regulates NK cytotoxicity and anti-tumor immune response against GC cells by inducing ferroptosis.

Ferroptosis relies on the intersection of iron, thiol, and lipid metabolic pathways [17,48]. Our observations suggested that CAFs augment the labile iron pool in NK cells through two pathways: one originating from CAFs' iron metabolism and the other from NK cells' iron metabolism (Fig. 7) On the one hand, CAFs could export iron into the TME, which is accompanied by the upregulation of iron regulatory genes FPN1 and HEPH. We demonstrated that treatment of CAFs with iron chelators DFP or DFO significantly reduces the NK cell labile iron pool and suppresses CAF-induced ferroptosis, thereby confirming the role of CAFs in disturbing the iron homeostasis in NK cells. On the other hand, intracellular iron homeostasis involves the coordination between iron export, import, and storage [49]. We demonstrated that CAFs elevate the expression of NCOA4, a specific cargo receptor implicated in the degradation of ferritin within autophagosomes (ferritinophagy), in NK cells [30]. Under normal physiological conditions, ferritinophagy is precisely regulated by an iron-dependent protein network [30]; however, excessive ferritinophagy can lead to ferroptosis [50]. Thus, our identification of NCOA4 as a target gene for CAFs response is consistent with a role for NK cell ferroptosis induced by CAFs. We also determined that CAF-derived FSTL1 upregulates NCOA4 expression in NK cells via the DIP2A-P38 pathway. The p38 MAPK pathway has previously been reported as an upstream regulatory signaling pathway of NCOA4 [40], and this study provides an important mechanistic link to explain its role in GC. We demonstrated that CAF-derived FSTL1 also plays a crucial role in inducing NCOA4 mediated-ferritinophagy in NK cells. Thus, blocking the secretion of FSTL1 by CAFs provides an additional viable strategy for improving NK cell cytotoxicity in GC.

Given the above evidence for CAF-induced NK cell ferroptosis and FSTL1-NCOA4-mediated ferritinophagy, we evaluated a combined approach for GC treatment involving concurrent application of DFO and FSTL1-neutralizing antibody. As anticipated, this combination effectively suppresses ferroptosis in NK cells, which enhances NK cell cytotoxicity. For further assessment of this strategy, we employed CAR-NK cells, which are therapeutically effective for hematological and non-hematological malignancies but are limited by sub-optimal outcomes for solid tumors due to immunosuppressive signals from tumor stroma [12]. Our results showed that the addition of DFO and FSTL1-neutralizing antibody enhances MSLN-CAR-NK cell cytotoxicity against GC cells, which further supports the mechanism of CAF-induced ferroptosis in NK cells.

In summary, our study provides valuable insights into the interplay between CAFs and NK cells in GC. CAFs increase labile iron within NK cells to induce ferroptosis by exporting iron into the TME and promoting FSTL1-NCOA4-mediated ferritinophagy. Our findings emphasize the potential of targeting these pathways as a therapeutic strategy to enhance the immune response of NK cells against GC. However, further investigation is warranted in order to understand the intricate interactions between CAFs and immune cells in the TME and explore the clinical implications of these findings for the treatment of GC.

Data availability statement

All data and material will be made available upon request.

Declaration of competing interest

The authors declare that there are no competing financial interests in relation to the work described.

Acknowledgements

We thank LetPub (www.letpub.com) for linguistic assistance and pre-submission expert review. This work was supported by the National Natural Science Foundation of China (Nos. 82072616, 82273266, 82203606, 82103392), Shanghai Municipal Education Commission-Gaofeng Clinical Medicine Grant Support (No. 20152505), Natural Science Foundation of Shanghai (No. 23ZR1440000).

Appendix A. Supplementary data

Supplementary data to this article can be found online at https://doi.org/10.1016/j.redox.2023.102923.

References

[1] H. Sung, et al., Global cancer statistics 2020: GLOBOCAN estimates of incidence and mortality worldwide for 36 cancers in 185 countries, CA A Cancer J. Clin. 71 (3) (2021) 209–249.
[2] N. Kemi, et al., Tumour-stroma ratio and prognosis in gastric adenocarcinoma, Br. J. Cancer 119 (4) (2018) 435–439.
[3] C. Walker, E. Mojares, A. Del Río Hernández, Role of extracellular matrix in development and cancer progression, Int. J. Mol. Sci. 19 (10) (2018).
[4] T.K. Mak, et al., The cancer-associated fibroblast-related signature predicts prognosis and indicates immune microenvironment infiltration in gastric cancer, Front. Immunol. 13 (2022), 951214.
[5] Y. Zavros, J.L. Merchant, The immune microenvironment in gastric adenocarcinoma, Nat. Rev. Gastroenterol. Hepatol. 19 (7) (2022) 451–467.
[6] E.A. De Jaeghere, H.G. Denys, O. De Wever, Fibroblasts fuel immune escape in the tumor microenvironment, Trends Cancer 5 (11) (2019) 704–723.
[7] M.A. Cooper, T.A. Fehniger, M.A. Caligiuri, The biology of human natural killer-cell subsets, Trends Immunol. 22 (11) (2001) 633–640.
[8] A.M. Abel, et al., Natural killer cells: development, maturation, and clinical utilization, Front. Immunol. 9 (2018) 1869.
[9] C. Guillerey, N.D. Huntington, M.J. Smyth, Targeting natural killer cells in cancer immunotherapy, Nat. Immunol. 17 (9) (2016) 1025–1036.
[10] J.Y. Kim, et al., Increase of NKG2D ligands and sensitivity to NK cell-mediated cytotoxicity of tumor cells by heat shock and ionizing radiation, Exp. Mol. Med. 38 (5) (2006) 474–484.
[11] E. Liu, et al., Use of CAR-transduced natural killer cells in CD19-positive lymphoid tumors, N. Engl. J. Med. 382 (6) (2020) 545–553.
[12] E. Wrona, M. Borowiec, P. Potemski, CAR-NK cells in the treatment of solid tumors, Int. J. Mol. Sci. 22 (11) (2021).
[13] K. Pan, et al., CAR race to cancer immunotherapy: from CAR T, CAR NK to CAR macrophage therapy, J. Exp. Clin. Cancer Res. 41 (1) (2022) 119.
[14] K.M. Maalej, et al., CAR-cell therapy in the era of solid tumor treatment: current challenges and emerging therapeutic advances, Mol. Cancer 22 (1) (2023) 20.
[15] M. Vitale, et al., Effect of tumor cells and tumor microenvironment on NK-cell function, Eur. J. Immunol. 44 (6) (2014) 1582–1592.
[16] T. Li, et al., Hepatocellular carcinoma-associated fibroblasts trigger NK cell dysfunction via PGE2 and Ido, Cancer Lett. 318 (2) (2012) 154–161.
[17] D. Li, Y. Li, The interaction between ferroptosis and lipid metabolism in cancer, Signal Transduct. Targeted Ther. 5 (1) (2020) 108.
[18] X. Wu, et al., Hepatocyte growth factor activates tumor stromal fibroblasts to promote tumorigenesis in gastric cancer, Cancer Lett. 335 (1) (2013) 128–135.
[19] Z. Jin, et al., The cross-talk between tumor cells and activated fibroblasts mediated by lactate/BDNF/TrkB signaling promotes acquired resistance to anlotinib in human gastric cancer, Redox Biol. 46 (2021), 102076.
[20] Y. Bentur, M. McGuigan, G. Koren, Deferoxamine (desferrioxamine). New toxicities for an old drug, Drug Saf. 6 (1) (1991) 37–46.
[21] D.H. Manz, et al., Iron and cancer: recent insights, Ann. N. Y. Acad. Sci. 1368 (1) (2016) 149–161.
[22] L. Shen, et al., Crosstalk between macrophages, T cells, and iron metabolism in tumor microenvironment, Oxid. Med. Cell. Longev. (2021), 8865791, 2021.
[23] H.I. Atiya, et al., Endometriosis-associated mesenchymal stem cells support ovarian clear cell carcinoma through iron regulation, Cancer Res. 82 (24) (2022) 4680–4693.
[24] D. Vela, Iron in the tumor microenvironment, Adv. Exp. Med. Biol. 1259 (2020) 39–51.

[25] A. Donovan, et al., The iron exporter ferroportin/Slc40a1 is essential for iron homeostasis, Cell Metabol. 1 (3) (2005) 191–200.
[26] J. Petrak, D. Vyoral, Hephaestin–a ferroxidase of cellular iron export, Int. J. Biochem. Cell Biol. 37 (6) (2005) 1173–1178.
[27] R.C. Hider, A.V. Hoffbrand, The role of deferiprone in iron chelation, N. Engl. J. Med. 379 (22) (2018) 2140–2150.
[28] U. Testa, E. Pelosi, C. Peschle, The transferrin receptor, Crit. Rev. Oncog. 4 (3) (1993) 241–276.
[29] M. Worwood, Ferritin, Blood Rev. 4 (4) (1990) 259–269.
[30] J.D. Mancias, et al., Quantitative proteomics identifies NCOA4 as the cargo receptor mediating ferritinophagy, Nature 509 (7498) (2014) 105–109.
[31] A. Mattiotti, et al., Follistatin-like 1 in development and human diseases, Cell. Mol. Life Sci. 75 (13) (2018) 2339–2354.
[32] N. Ouchi, et al., DIP2A functions as a FSTL1 receptor, J. Biol. Chem. 285 (10) (2010) 7127–7134.
[33] J. Xu, et al., Fstl1 antagonizes BMP signaling and regulates ureter development, PLoS One 7 (4) (2012), e32554.
[34] K. Murakami, et al., Follistatin-related protein/follistatin-like 1 evokes an innate immune response via CD14 and toll-like receptor 4, FEBS Lett. 586 (4) (2012) 319–324.
[35] W. Chen, et al., Follistatin-like 1 protects cardiomyoblasts from injury induced by sodium nitroprusside through modulating Akt and Smad1/5/9 signaling, Biochem. Biophys. Res. Commun. 469 (3) (2016) 418–423.
[36] J. Chiou, et al., Decrease of FSTL1-BMP4-Smad signaling predicts poor prognosis in lung adenocarcinoma but not in squamous cell carcinoma, Sci. Rep. 7 (1) (2017) 9830.
[37] D. Fang, et al., Ups and downs: the PPARγ/p-PPARγ seesaw of follistatin-like 1 and integrin receptor signaling in adipogenesis, Mol. Metabol. 55 (2022), 101400.
[38] J. Guo, et al., Knockdown of FSTL1 inhibits oxLDL-induced inflammation responses through the TLR4/MyD88/NF-κB and MAPK pathway, Biochem. Biophys. Res. Commun. 478 (4) (2016) 1528–1533.
[39] M. Wu, et al., FSTL1 promotes growth and metastasis in gastric cancer by activating AKT related pathway and predicts poor survival, Am. J. Cancer Res. 11 (3) (2021) 712–728.
[40] Z. Wu, et al., High-dose ionizing radiation accelerates atherosclerotic plaque progression by regulating P38/NCOA4-mediated ferritinophagy/ferroptosis of endothelial cells, Int. J. Radiat. Oncol. Biol. Phys. (2023).
[41] M. Zhu, et al., STAT3 signaling promotes cardiac injury by upregulating NCOA4-mediated ferritinophagy and ferroptosis in high-fat-diet fed mice, Free Radic. Biol. Med. 201 (2023) 111–125.
[42] M. Sotoudeh, et al., MSLN (Mesothelin), ANTXR1 (TEM8), and MUC3A are the potent antigenic targets for CAR T cell therapy of gastric adenocarcinoma, J. Cell. Biochem. 120 (4) (2019) 5010–5017.
[43] M. Grönholm, et al., Patient-derived organoids for precision cancer immunotherapy, Cancer Res. 81 (12) (2021) 3149–3155.
[44] E. Driehuis, K. Kretzschmar, H. Clevers, Establishment of patient-derived cancer organoids for drug-screening applications, Nat. Protoc. 15 (10) (2020) 3380–3409.
[45] G.J. Yoshida, Applications of patient-derived tumor xenograft models and tumor organoids, J. Hematol. Oncol. 13 (1) (2020) 4.
[46] M. Balsamo, et al., Melanoma-associated fibroblasts modulate NK cell phenotype and antitumor cytotoxicity, Proc. Natl. Acad. Sci. U. S. A. 106 (49) (2009) 20847–20852.
[47] L. Ziani, et al., Melanoma-associated fibroblasts decrease tumor cell susceptibility to NK cell-mediated killing through matrix-metalloproteinases secretion, Oncotarget 8 (12) (2017) 19780–19794.
[48] J. Zheng, M. Conrad, The metabolic underpinnings of ferroptosis, Cell Metabol. 32 (6) (2020) 920–937.
[49] G. Vigani, et al., Essential and detrimental - an update on intracellular iron trafficking and homeostasis, Plant Cell Physiol. 60 (7) (2019) 1420–1439.
[50] N. Santana-Codina, J.D. Mancias, The role of NCOA4-mediated ferritinophagy in health and disease, Pharmaceuticals 11 (4) (2018).